

New amorphous silicon majority-carrier device

Jin Jang and Choochon Lee

Citation: [Applied Physics Letters](#) **43**, 90 (1983); doi: 10.1063/1.94133

View online: <http://dx.doi.org/10.1063/1.94133>

View Table of Contents: <http://scitation.aip.org/content/aip/journal/apl/43/1?ver=pdfcov>

Published by the [AIP Publishing](#)

Articles you may be interested in

[Majority-carrier diffusion coefficients in degenerately doped silicon](#)

J. Appl. Phys. **62**, 3809 (1987); 10.1063/1.339221

[Anomalous majority-carrier peaks in deep level transient spectroscopy](#)

J. Appl. Phys. **59**, 168 (1986); 10.1063/1.336856

[Modulated barrier photodiode: A new majority-carrier photodetector](#)

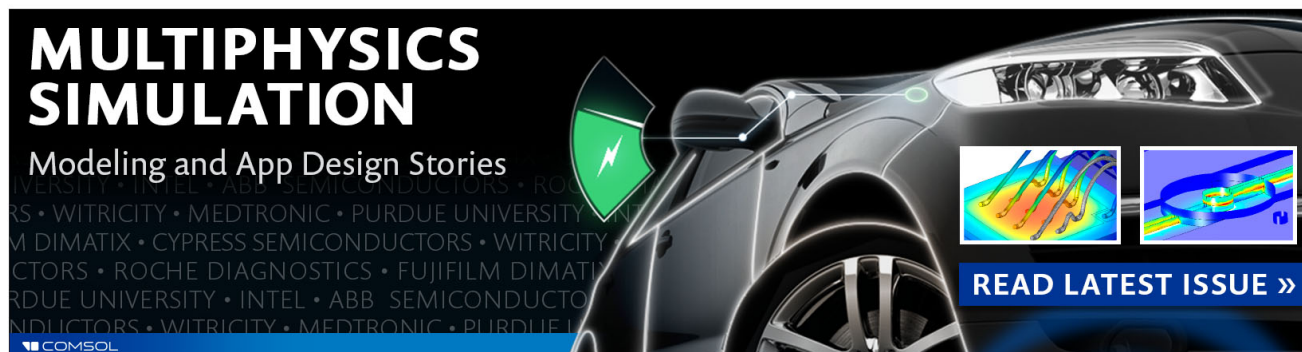
Appl. Phys. Lett. **39**, 340 (1981); 10.1063/1.92715

[A majority-carrier camel diode](#)

Appl. Phys. Lett. **35**, 63 (1979); 10.1063/1.90931

[Acoustic-surface-wave measured majority-carrier surface mobilities](#)

J. Appl. Phys. **46**, 3205 (1975); 10.1063/1.321973

The advertisement features a dark background with a sleek, modern car. On the left, the text 'MULTIPHYSICS SIMULATION' is written in large, bold, white letters. Below it, 'Modeling and App Design Stories' is written in a smaller white font. A green lightning bolt icon is positioned to the right of the text. In the bottom left corner, the COMSOL logo is visible. On the right side, there are two small inset images showing simulation results: one with a blue and yellow color map and another with a blue and red color map. At the bottom right, a blue button with white text says 'READ LATEST ISSUE >>'. The background also contains faint, repeating text of various company names like 'INTEL', 'ABB', 'SEMICONDUCTORS', 'ROCHE', 'MEDTRONIC', 'PURDUE UNIVERSITY', 'DIMATIX', 'CYPRESS SEMICONDUCTORS', 'FUJIFILM DIMATIX', 'RDUE UNIVERSITY', 'INTEL', 'ABB', 'SEMICONDUCTORS', 'NDUCTORS', 'WITRICITY', 'MEDTRONIC', 'PURDUE U'.

New amorphous silicon majority-carrier device

Jin Jang

Department of Physics, Kyung Hee University, Dongdaemoon-Gu, Seoul, Korea

Choochon Lee

Department of Physics, Korea Advanced Institute of Science and Technology, P. O. Box 150 Chongyangni, Seoul, Korea

(Received 18 January 1983; accepted for publication 10 April 1983)

A new majority-carrier rectifying device is demonstrated which is made in hydrogenated amorphous silicon deposited by glow discharge decomposition. The devices were made in a structure composed of phosphorus doped, boron doped, intrinsic, and phosphorus-doped layers in series, prepared by using doping gas in the discharge. The rectification ratio at 1 V is over 10^6 . Barrier heights depend on the thickness of boron-doped layer, and barriers as high as 1.09 eV are obtained with boron-doped layer of 120 Å. Conversion efficiencies of up to 5.7% under 20-mW/cm² illumination have been observed.

PACS numbers: 85.30.Kk

Hydrogenated amorphous silicon (*a*-Si:H) produced from the glow discharge decomposition of silane has been studied extensively in recent years.¹ Thin-film photovoltaic devices have been fabricated with these materials in Schottky barrier, metal-insulator-semiconductor (MIS), and *p-i-n* (or *n-i-p*) configurations, where *p* represents *p* type, *i* intrinsic, and *n* *n*-type amorphous silicons, with conversion efficiencies of up to 5.5,² 6.3,³ and 8.0%,⁴ respectively.

Majority-carrier diodes are important components in electronic circuits because current transport is not restricted by the diffusion of minority carriers, and the potential drop across a device can be significantly smaller than for corresponding *p-i-n* or *p-n* junction devices operating at the same current level. A non-Schottky, majority-carrier diode called a camel diode, in which the current transport is controlled by a potential barrier in the bulk of the semiconductor, was reported by Shannon.⁵

In this letter we demonstrate a new majority-carrier device composed of hydrogenated amorphous silicon, which shows good rectifying and photovoltaic behavior.

Our devices were fabricated by depositing glow discharge-produced *a*-Si:H on the substrates of indium-tin-oxide (ITO) coated glass at substrate temperature of 250 °C. The surface resistivity of the ITO coating was 20 Ω/□. The device structure is shown in Fig. 1(a). Full details concerning the conditions required for deposition have been given elsewhere.⁶ A thin, highly doped *n* layer (250 °C) was deposited onto an ITO coated glass by the discharge of 1.0 vol. % phosphine mixed silane gas. Next, an 80–200-Å-thick *p* layer was deposited using a volume gas ratio of B₂H₆/SiH₄ = 0.7%. Then, a 6000-Å-thick layer of undoped *a*-Si:H was deposited by the decomposition of pure silane. Then, a 250-Å-thick *n* layer was prepared using a volume gas ratio of PH₃/SiH₄ = 1.0%. Finally, a layer of ~1000-Å-thick evaporated Al film served as the back electrode.

The energy-band diagram of the *a*-Si:H *n-p-i-n* camel diodes is shown schematically in Fig. 1(b). The conduction and valence bands, *E_c* and *E_v*, refer respectively to the electron-extended and hole-extended states of *a*-Si:H. The barrier region, the width of which depends on the density of states in the gap of undoped *a*-Si:H, extends through a frac-

tion of the layer, and the distance of the Fermi level from *E_c* in the bulk is *E_F*. *N_a* and *N_d* are the ionized centers close to the extended states, and the deep lying centers which ionize in the barrier region are also indicated. The holes trapped in the potential minimum are also shown in Fig. 1(b). It is possible to control the height of the potential barrier by the thickness of the *p* layer.

The barrier height is ϕ_B and the built-in potential is V_0 . The current-voltage (*I-V*) relation for rectifying diodes under forward bias can be written in the form

$$j = j_s [\exp(eV/nkT) - 1], \quad (1)$$

where *j_s* is the saturation current density, *V* is the applied voltage, and *n* is the diode quality factor. The values of *n* are generally close to unity, but can lie between 1 and 2 if there is recombination in the barrier or if there is a thin insulating layer at the interface.

Because of the short mean free paths in *a*-Si:H films the diffusion theory of rectification rather than the thermionic

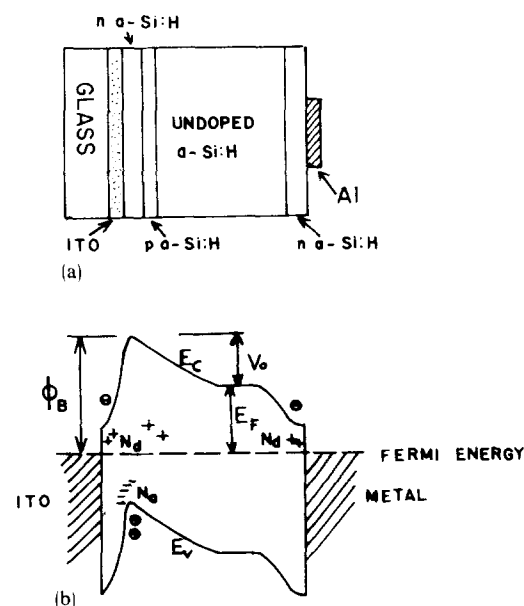


FIG. 1. (a) Schematic diagram of the structure used in the study of *a*-Si:H *n-p-i-n* devices. (b) Energy-band diagram of the *a*-Si:H *n-p-i-n* diode.

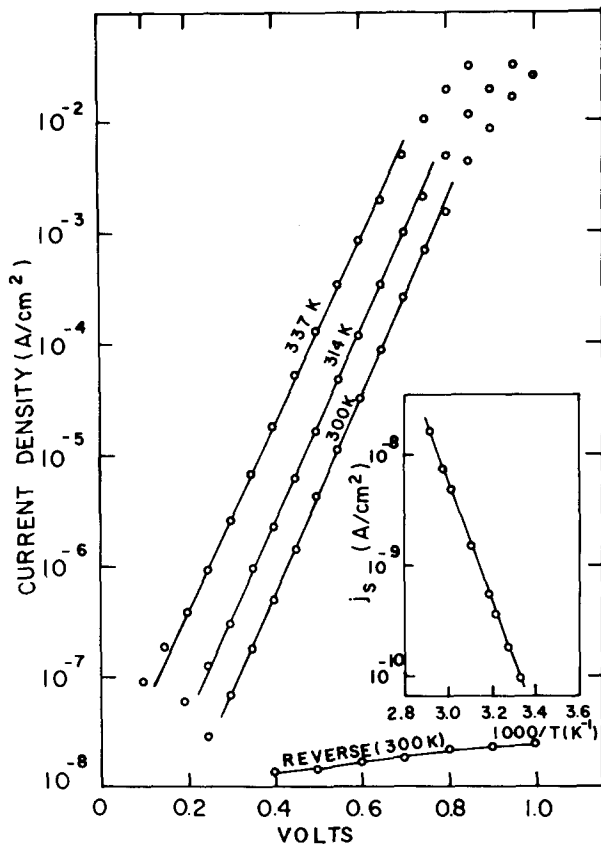


FIG. 2. Forward bias currents of an *a*-Si:H *n-p-i-n* diode at several temperatures. The inset shows the temperature dependence of the extrapolated values of j_s .

theory can be applicable. The saturation current density is then given by⁸

$$j_s = q \mu_c N_c E_m \exp(-\phi_B/kT), \quad (2)$$

where μ_c is the electron mobility, E_m is the maximum electric field in the *i* layer, and N_c is the effective density of states in the conduction band.

The *I-V* characteristics of *a*-Si:H *n-p-i-n* barriers have the same form as those of Schottky barrier and *p-i-n* diodes. Under far forward bias, the currents become series resistance limited. The current in far forward does not show Ohmic, but space-charge-limited behavior. Under reverse bias the currents have a saturated form, and rectification ratios $\geq 10^6$ are obtained at 1 V for *a*-Si:H *n-p-i-n* devices with *p*-layer thickness of 120 Å.

The forward-bias *I-V* characteristics of the *n-p-i-n* de-

TABLE I. Static and transport diode parameters as a function of the thickness of the *p* layer in *n-p-i-n* diodes. The parameters are the open circuit voltage V_{oc} at 20 mW/cm², the nonideality factor *n*, and the barrier height ϕ_B .

<i>p</i> -layer thickness (Å)	<i>n</i>	V_{oc} (V)	ϕ_B (eV)
80	1.34	0.40	0.82
100	1.46	0.53	0.94
120	1.80	0.69	1.09
200	1.94	0.38	0.80

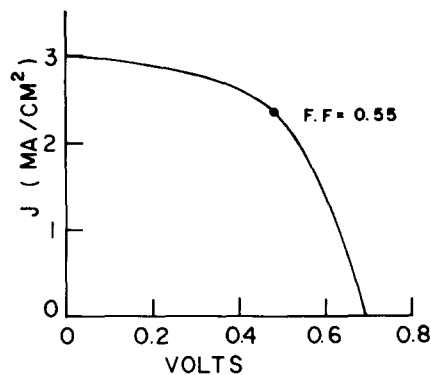


FIG. 3. Illuminated *I-V* characteristics of ITO/*n-p-i-n* device with *p*-layer thickness of 120 Å under 20-mW/cm² sunlight.

vice with *p*-layer thickness of 120 Å measured at various temperatures are shown in Fig. 2. The currents at all temperatures satisfy Eq. (1) with $n = 1.80$. The extrapolated current densities j_s increase with temperature (this is shown in the inset of Fig. 2) and satisfy Eq. (2), where $\phi_B = 1.09$ eV and $q \mu_c N_c E_m = 1.8 \times 10^8$ A/cm². If the values $\mu_c = 10$ cm²/Vs and $N_c = 1 \times 10^{21}$ cm⁻³ (Ref. 9) are used, $E_m = 1.1 \times 10^5$ V/cm is obtained.

The diode parameters obtained from the temperature dependence of forward current densities were observed to depend strongly on the thickness of *p* layer in *a*-Si:H camel devices. The summary of device parameters for the various *p*-layer thicknesses is shown in Table I. As the thickness of the *p* layer is increased from 80 to 200 Å, the diode quality factor increases from 1.34 up to 1.94. However, as the thickness of the *p* layer is increased, the barrier height and open circuit voltage increase, and have maximum values at the thickness of 120 Å, and then decrease (see Table I). This can be explained by the fact that as the thickness of the *p* layer is increased above 120 Å, the number of holes trapped in the potential minimum is increased, resulting in the decrease of barrier height and open circuit voltage. The increase of trapped holes in the potential minimum gives rise to the increase of the tunneling currents through the *p* layer, resulting in the increase of the diode quality factor. The optimum thickness of the *p* layer in *a*-Si:H camel diodes was observed to be 100–120 Å. However, the optimum thickness depends on the densities of ionized acceptors and defects in the *p* layer.

In Fig. 3 we show the illuminated *I-V* characteristics for a *n-p-i-n* device with *p*-layer thickness of 120 Å as measured at the sunlight of 20-mW/cm² incident power density. The characteristics of the device are open circuit voltage $V_{oc} = 0.69$ V, short circuit current density $J_{sc} = 3.0$ mA/cm², fill factor of 0.55, and conversion efficiency of 5.7%. The area of the device is 3.0 mm². This efficiency has been reproduced in several cells.

To compare the photovoltaic properties of *n-p-i-n* with those of *p-i-n* cells, we fabricated *p-i-n* devices under the same deposition conditions as those for the deposition of *n-p-i-n* cells. In *p-i-n* device we take the thicknesses of *p*, *i*, and *n* layers to be 120, 6000, and 250 Å, respectively, using the same gas mixtures as those used to prepare *n-p-i-n* devices.

The characteristics of the $p-i-n$ devices are $V_{oc} = 0.71$ V, $J_{sc} = 3.5$ mA/cm², fill factor of 0.50, and efficiency of 6.2%. The area of this cell is 3.0 mm.² Although the fill factor of the $n-p-i-n$ device is higher than that of the $p-i-n$ cell, the efficiency of the $n-p-i-n$ device is lower than that of the $p-i-n$ cell because of the ineffective collection of carriers generated at the front n layer. If phosphorus-doped amorphous silicon carbide, which has wide band gap and good photoconductivity,¹⁰ is substituted for the front n layer in ITO/ $n-p-i-n$ cells, the conversion efficiencies of $n-p-i-n$ cells will be increased. To increase the barrier heights of a -Si:H $n-p-i-n$ devices, the wide band-gap p -type material such as the amorphous silicon carbide doped with boron is suggested to be used for the p layer in $n-p-i-n$ devices.

In conclusion, we have presented the evidence that the $n-p-i-n$ devices fabricated from discharge-produced a -Si:H have good rectifying and photovoltaic properties.

This research was supported by the Ministry of Science and Technology, Korea, under contract No. 4N-00034. Final support is appreciated very much.

- ¹See, e.g., H. Fritzsche, *Solar Energy Mater.* **3**, 447 (1980).
²D. E. Carlson and C. R. Wronski, *J. Electron. Mater.* **6**, 95 (1977).
³A. Madan, J. McGill, W. Czubatyl, J. Yang, and S. R. Ovshinsky, *Appl. Phys. Lett.* **37**, 826 (1980).
⁴Y. Tawada, K. Tsuge, M. Kondo, H. Okamoto, and Y. Hamakawa, *J. Appl. Phys.* **53**, 5273 (1982).
⁵J. M. Shannon, *Appl. Phys. Lett.* **35**, 63 (1978).
⁶J. Jang and C. Lee, *Solar Energy Mater.* **7**, 377 (1982).
⁷E. H. Rhoderick, *Metal Semiconductor Contacts* (Clarendon, Oxford, 1978).
⁸E. Spence, *Electronic Semiconductors* (McGraw-Hill, New York, 1958).
⁹A. Madan, S. R. Ovshinsky, and E. Benn, *Philos. Mag.* **B 40**, 259 (1979).
¹⁰Y. Tawada, M. Kondo, H. Okamoto, and Y. Hamakawa, *Solar Energy Mater.* **6**, 299 (1982).

Crystallographic orientation of laser-recrystallized Ge films on fused quartz

Takashi Nishioka, Yukinobu Shinoda, and Yoshiro Ohmachi

Musashino Electrical Communication Laboratory, Nippon Telegraph and Telephone Public Corporation, Musashino-shi, Tokyo 180, Japan

(Received 23 March 1983; accepted for publication 10 April 1983)

Crystallographic orientation of laser-recrystallized Ge films on fused quartz has been investigated using a microprobe x-ray diffractometer (μ XD) that has a collimated x-ray beam of 30 μ m in diameter and a position-sensitive proportional counter. It has been found that the crystallographic orientations normal to the substrate surface were near $\langle 110 \rangle$ or $\langle 111 \rangle$. Tilt angle of the grain from $\langle 110 \rangle$ or $\langle 111 \rangle$ was $\leq 10^\circ$. Orientation distribution was represented by means of a stereographic projection.

PACS numbers: 81.10.Jt

A considerable amount of work has been carried out recently on the crystallization of semiconductor films on amorphous insulating substrates in the attempt to achieve large-area display circuits or three-dimensional integrated circuits. Several techniques, such as laser¹⁻³ or electron-beam⁴ irradiation and zone melting using a movable graphite heater,⁵ have been reported to prepare silicon-on-insulator (SOI) structures.

Information regarding crystallographic orientation or defects in recrystallized films, or concerning electrical properties at the grain boundaries is important for obtaining high-quality devices. This letter presents the results of investigation by means of a microprobe x-ray diffractometer (μ XD) into the crystallographic orientation of laser-recrystallized Ge films on fused quartz. The crystallographic properties of the recrystallized Si films have previously been investigated through etch-pit formation using anisotropic chemical etching,⁶ as well as microprobe reflection high-energy electron diffraction.⁷ These techniques, however, necessitate either a photolithographic process or somewhat complicated diffraction pattern analysis. The μ XD technique presented here provides a simple, nondestructive

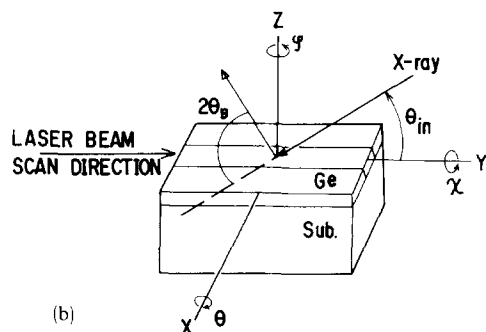
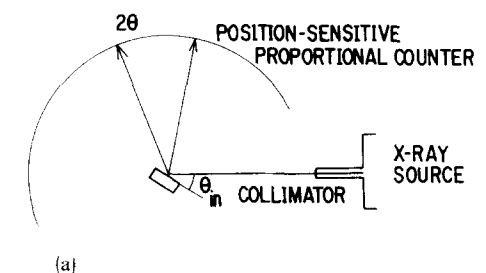


FIG. 1. Schematic illustrations of (a) μ XD apparatus and (b) rotation axes of the system.